

De-asymmetry Method for Distribution Function of Fiber Orientation in Injection Molded Composites

Shanjie Zhi^{*}, Xizhou Yang^{**}, Xintian Liu^{**} and Hejian Liu^{*}

Keywords: fiber orientation distribution, mechanical properties, Weibull distribution, injection molded composites.

ABSTRACT

Fiber orientation is a key factor in determining the mechanical properties of injection molded composites. Therefore, accurate description of fiber orientation plays an important role in the performance evaluation of injection molded composites. The relationship between the effective thickness in the thickness direction and the probability density of the fiber orientation tensor is built up. Based on it, a smooth segmented linear function of fiber orientation is proposed to obtain the cumulative distribution function of fiber orientation tensor. Considering the asymmetry and non-monotonicity of the fiber orientation distribution, a de-asymmetry method is proposed. Compared with the experimental results in the literature, the cumulative distribution function has a good fit, and the experimental results correlate well with the elastic modulus obtained by the de-asymmetry method. It could provide a reference basis for subsequent studies based on the thickness distribution of the fiber orientation tensor.

INTRODUCTION

With low specific gravity and high specific strength and modulus, composites exhibit excellent mechanical properties and processability. And fiber reinforced composites have higher impact resistance, strength, stiffness, enhanced creep and fatigue

resistance compared to short-fiber materials (Truckenmüller and Fritz, 1991; Wang et al., 2022; Liu et al., 2022). Among such materials, long fiber-reinforced thermoplastics (LFTs) are more widely used in structural weight reduction, which are composed of a thermoplastic polymer matrix and a discontinuous fiber reinforcement base exceeding a critical fiber length-to-diameter ratio (Ning et al., 2019). The injection molding equipment can be used for the production of LFTs with minor modifications, thus LFTs presenting low-cost characteristics compared to other composites. These advantages make LFTs one of the most advanced lightweight engineering materials.

For LFT products, the main factors affecting the mechanical properties include the retention length of the fibers, the orientation state of the fibers, and the distribution density of the fibers (fiber volume fraction) in the part. What's more, fiber volume fraction can be artificially controlled. Therefore, it is important to analyze the retention length and orientation state of fibers to study the mechanical properties of LFT.

Since the birth of composite materials, their microstructure has been continuously studied and the internal structure of composite products has been observed with the help of techniques such as scanning electron microscopy (SEM) and x-ray computed tomography (uCT) (Friedrich, 1998; Hessman et al., 2019; Chang et al., 2020; Laspalas et al., 2008). And image-based methods for microstructure reduction and analysis of composite materials have been developed and improved over the decades. There has also been some progress in research on fatigue (Kebir, T., et al., 2021; Viana, C.O., et al., 2021).

In general, it is believed that LFTs exhibit a shell-core-shell three-layer sandwich structure along their thickness direction. And the fiber orientation changes gradually from the core region to the shell region. It has also been suggested that LFTs exhibit a five-layer sandwich-type structure of skin-shell-core-shell-skin along their thickness direction (Tseng et al., 2020). Although the structural forms of the described

*Paper Received October, 2022. Revised December, 2022.
Accepted December, 2022. Author for Correspondence: Xintian Liu*

**Applied Technology College of Soochow University*

***School of Mechanical and Automotive Engineering, Shanghai University of Engineering Science, Shanghai 201620, China*

composites are largely consistent when the fundamentals are explored.

Based on the layered structure of the composite material observed by scanning electron microscopy technique, as shown in Figure 1(a) for the thin plate injection molding structure model, the layered structure of the injection molded composite material is generally considered to be symmetrical along the center of the thickness in theory. In Figure 1(a), t refers to the thickness of the composite specimen, t_c refers to the thickness of the core region, and t_s refers to the thickness of the shell region. For the convenience of representation, the ratio of the thickness of the core region to the thickness of the specimen (h_c) and the ratio of the thickness of the shell region to the thickness of the specimen (h_s) are used to denote the structural properties as follows:

$$\begin{cases} h_c = t_c/t \\ h_s = t_s/t \\ h_c + h_s = 1 \end{cases} \quad (1)$$

THEORETICAL FRAMEWORKS

Fiber Orientation Tensor

The fiber orientation state of discontinuous fiber reinforced material can be described by the fiber orientation tensor defined by Advani and Tucker (Advani and Tucker, 1987). For a single fiber, considered as a rigid cylindrical rod, the spatial state is described by a unit vector p . Previous authors described this unit vector in terms of three Euler angles. Advani and Tucker reduced it to two variables, as shown in Figure 1(c). And the final expression for the unit vector p is given by:

$$p = \begin{pmatrix} \cos\theta \\ \sin\theta \cos\phi \\ \sin\theta \sin\phi \end{pmatrix} \quad (2)$$

Considering all fibers in the study area, all possible orientations of these fibers constitute a probability space ψ , which is named the probability density function (PDF) $\psi(p)$. It indicates the probability of the fibers in the orientation taken. For the whole probability space, the sum of all fiber orientation possibilities is 1, which corresponds to the mathematical form $\oint \psi(p) dp = 1$, called the normalization requirement.

Defining the unit vector p based on the orientation space and vector for the fiber orientation tensor A , which is used to describe the numerical calculation of the fiber orientation theoretical model in engineering applications. A is a symmetric second-order tensor with a trace of 1 and $A = \oint \psi(p) p p dp$. Using the tensor representation, it can be expressed as:

$$A_{ij} = \int \psi(p) p_i p_j dp \quad (3)$$

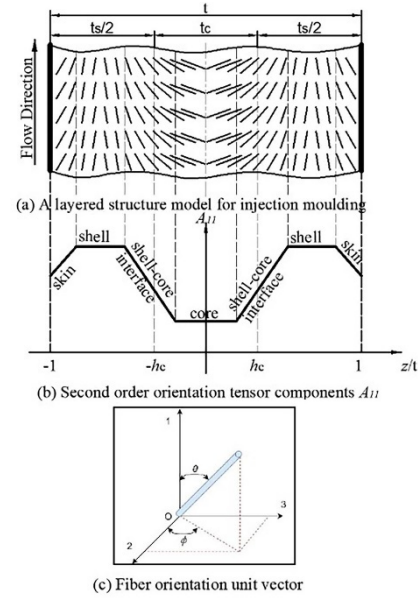


Figure 1 Thin plate injection molding structure model and fiber orientation schematic

denoted as $A_{ij} = \langle p_i p_j \rangle$, which represents the average amount in a certain volume region. The second-order tensor A has nine components to describe fibers at a certain location. When discussing the results of fiber orientation of a standard block or some other simple geometry of injection molded parts, it is generally considered that subscript 1 represents the flow direction, subscript 2 represents the lateral direction of flow, and the subscript 3 represents the thickness direction. And the corresponding fiber orientation tensor is A_{11}, A_{22}, A_{33} . The magnitude of the value of A_{ii} represents the degree of fiber orientation in this direction, and a larger value indicates that the fibers tend to be more aligned in this direction, while a smaller value indicates that they tend to be less aligned. When its value is 1, the fibers are perfectly neatly aligned. Figure 1(b) represents the values of the fiber orientation tensor taken for different fiber orientation states.

In the past decades, some theoretical models of suspension rheology have been proposed to predict the fiber orientation distribution. The general form of ellipsoidal particle orientation in Newtonian fluids under the action of the flow field was proposed (Jeffery, 1922), which is generally known as Jeffery model. And this model was the origin for the study of fiber orientation, but the particles of this model are more easily oriented than the actual situation. Subsequently, the interaction factor to describe the effect of interaction between fibers on fiber orientation was introduced to Jeffery model. The Folgar-Tucker model (F-T model) which was proposed (Folgar and Tucker, 1984), which is the first widely accepted and adopted model for fiber orientation. And the evolution of fiber orientation based on this model is faster than the actual one. Therefore, the Phelps-Tucker model was

proposed (Phelps and Tucker, 2009), considering the anisotropic rotational diffusion property. Then the iARD model was proposed (Tseng et al., 2016). Meanwhile, to reduce the kinetic evolution of fiber orientation, an external flux was introduced to the F-T model to stunt the fiber evolution and proposed the Reduced Strain Closure (RSC) model (Wang et al., 2008). And the image-only assumption of Intrinsic orientation dynamics (IOK) applied to describe the interaction between glass fibers and resin matrix and the RPR model was proposed. After that, the ARD-RSC (anisotropic rotary diffusion and reduced strain closure) model and the iARD-RPR (improved anisotropic rotary diffusion and retarding principal rate) models have also been proposed (Tseng et al., 2016). These advanced theoretical models have effectively contributed to the progress of fiber orientation prediction work.

Fiber Orientation Distribution Function

To date, there are many works of literatures discussion on PDFs in fiber orientation. And in recent years, a comprehensive review of typical fiber orientation distribution functions has been presented (Mishurova et al., 2018), among others.

A one-parameter exponential function was used to characterize the fiber orientation distribution in thin plate specimen pieces (Chin et al., 1988), and it is given as:

$$p(\theta; \lambda) = \frac{\lambda e^{-\lambda\theta}}{1 - e^{-\frac{\lambda\pi}{2}}}; 0 \leq \theta_{\min} \leq \theta \leq \theta_{\max} \leq \frac{\pi}{2} \quad (4)$$

Then, a combined function of Gaussian and triangular distributions was proposed to fit the distributions obtained from quantitative image analysis of SEM pictures (Lu and Liaw, 1995).

And a fiber orientation distribution function (Pettermann et al., 1997) was assumed as:

$$p(\theta; \lambda) = e^{-\frac{\theta^2}{2\lambda^2}} \quad (5)$$

Subsequently, shape parameters were used to describe the shape of the distribution curve with a two-parameter fiber orientation distribution function as (Fu and Lauke, 1998):

$$p(\theta) = \frac{(\sin \theta)^{2\alpha-1} (\cos \theta)^{2\beta-1}}{\int_{\theta_{\min}}^{\theta_{\max}} (\sin \theta)^{2\alpha-1} (\cos \theta)^{2\beta-1} d\theta}; 0 \leq \theta_{\min} \leq \theta \leq \theta_{\max} \leq \frac{\pi}{2} \quad (6)$$

where, α , β are shape parameters.

In 2000, considering the transversely isotropic orientation distribution of cracks, a fiber orientation distribution function of the following form was suggested (Sevostianov and Kachanov, 2000):

$$p(\theta; \lambda) = \frac{1}{2\pi} \left[(\lambda^2 + 1)e^{-\lambda\theta} + \lambda e^{-\frac{\lambda\pi}{2}} \right] \quad (7)$$

Equation (7) was later used to calculate the viscoelastic properties of short fiber reinforced composites (Sevostianov et al., 2016).

Clearly, these proposed typical fiber orientation distribution functions with only one waveform are not suitable for describing multiple wave forms resulting from sandwich-type layered microstructures of fiber orientation. And the current fiber orientation models cannot provide sufficiently accurate results. The following method will be proposed to apply to the multi-wave distribution.

Fiber Orientation Tensor Distribution Function

By analogy with the fiber orientation distribution function, this paper attempts to obtain the PDF of the fiber orientation tensor by starting from the cumulative distribution function (CDF) of the fiber orientation tensor A_{ii} . From this, the average fiber orientation tensor is obtained, and the mechanical properties of injection molded composites are predicted by homogenization methods.

The variation of the effective thickness z in the thickness direction is considered to be proportional to the probability density of the fiber orientation tensor, with the following relationship:

$$\frac{dz}{t} = p(A_{ii})dA_{ii} = P(A_{ii} + dA_{ii}) - P(A_{ii}) \quad (8)$$

$$dz = z(A_{ii} + dA_{ii}) - z(A_{ii}) \quad (9)$$

where $p(A_{ii})$ and $P(A_{ii})$ refer to the PDF and CDF of the fiber orientation tensor, respectively. And z refers to the position in the thickness direction, t refers to the total thickness of the sheet. A large number of data samples are usually required for analyzing PDFs. For example, to measure the fiber length distribution, a fiber sample of 2000 is given in the literature (Sharma et al., 2017). In contrast, smaller data is needed using the CDF.

The form of the distribution of the fiber orientation tensor along the thickness has shown in Figure 1(b), which can be approximated as a segmented linear function. In order to establish a good relationship between the segmented linear approximation function and the CDF, the segmented linear function is smoothed, which means that the experimentally obtained data are arranged from smallest to largest and the probability cumulative function is expressed in terms of the proportion of the occupied thicknesses according to the idea of Equation (8) and Equation (9). The specific steps are as follows:

- a) Combining the parts of the shell section close to the surface with the same tensor of its fiber orientation, which in fact means combining the proportion of the thickness occupied by the same tensor. This results in a change in the form of the

distribution of the fiber orientation tensor, as shown in Figure 2(a).

- b) Since the distribution of the fiber orientation tensor is theoretically symmetric, analyzing its negative proportional thickness part, the rearranged fiber orientation distribution is continuous, i.e., the first-order derivative of the CDF in Equation (8) is continuous. And the trend of the CDF can be established accordingly, as shown in Figure 2(b).

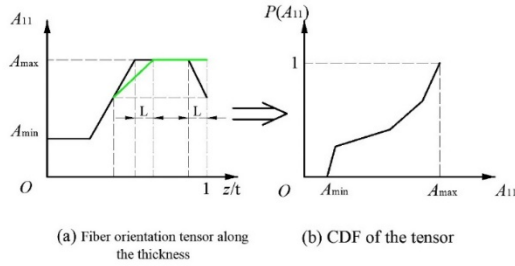


Figure 2 Processing for part of positive thickness ratio schematic

A generalized distribution function (GDF) was proposed for the fiber orientation distribution to fit data in the form of a double wave peak (Huang and Zhao, 2020). Extending its form to the fiber orientation tensor, taking A_{11} as an example, the lower the value of the fiber orientation tensor compared to the independent variable θ , the greater the angle of fiber orientation state, the more difficult it is to orient in the flow direction. It means that the generalized distribution function of the fiber orientation tensor has changed, and its expression is:

$$P(A_{11}) = (1 - h_s) \frac{1 - \exp\left(-\left(\frac{A_{11} - A_{\min}}{A_c}\right)^{\alpha_c}\right)}{1 - \exp\left(-\left(\frac{A_{\max} - A_{\min}}{A_c}\right)^{\alpha_c}\right)} + h_s \frac{\exp\left(-\left(\frac{A_{\max} - A_{11}}{A_s}\right)^{\alpha_s}\right) - \exp\left(-\left(\frac{A_{\max} - A_{\min}}{A_s}\right)^{\alpha_s}\right)}{1 - \exp\left(-\left(\frac{A_{\max} - A_{\min}}{\theta_s}\right)^{\alpha_s}\right)} \quad (10)$$

And the PDF which corresponds Equation (10) is:

$$p(A_{11}) = (1 - h_s) \frac{\frac{\alpha_c}{A_c} \left(\frac{A - A_{\min}}{A_c}\right)^{\alpha_c - 1} \exp\left(-\left(\frac{A - A_{\min}}{A_c}\right)^{\alpha_c}\right)}{1 - \exp\left(-\left(\frac{A_{\max} - A_{\min}}{A_s}\right)^{\alpha_c}\right)} + h_s \frac{\frac{\alpha_s}{A_s} \left(\frac{A_{\max} - A}{A_s}\right)^{\alpha_s - 1} \exp\left(-\left(\frac{A_{\max} - A}{A_s}\right)^{\alpha_s}\right)}{1 - \exp\left(-\left(\frac{A_{\max} - A_{\min}}{A_s}\right)^{\alpha_s}\right)} \quad (11)$$

similarly, where A_{\max} and A_{\min} are the maximum and minimum values of the experimental data respectively. and the shape parameters α_c , α_s and scale parameters θ_c , θ_s and h_s are the fit parameters. α_c , α_s , θ_c , θ_s are positive and $0 < h_s < 1$. An opposite trend is shown for the tensor A_{11} and A_{22} at the same position. Thus, the h_s in the Equations (10) and (11) should be

changed to h_c when the fitted objects are A_{22} .

De-asymmetry Method for Fiber Orientation Tensor

It is theoretically assumed that the variation of fiber orientation is distributed strictly symmetrically along its thickness center. In practice, however, the fiber orientation tensor is known to have a distribution that is not strictly symmetric. What's more, the variation of fiber orientation tensor in each layered structure is not monotonically varying. Based on the previous, the de-asymmetry method is proposed to better represent the relationship between the variation of the effective thickness t in the thickness direction and the probability density of the fiber orientation tensor.

The de-asymmetry method aims to reduce the influence of the approximately symmetric distribution and non-monotonic variation of fiber orientation on the final predicted elastic modulus, which is divided into two main categories: first, the experimental fiber orientation data are divided into two groups by the thickness of the center to avoid the influence of the symmetric distribution, and the results are fitted separately and then averaged; second, all the experimental data are arranged from small to large according to the idea of Equations (8) and (9). The cumulative distribution is used to fit the CDF of fiber orientation. These two types of methods are discussed below.

Method 1: Dividing the fiber orientation data into two groups from the thickness proper.

In this method, the form of the data to be processed is shown in Figure 3 and is divided into two main forms. Case 1 is the asymmetry (or approximate symmetry) due to the variation of fiber orientation at the outer boundary of the shell layer. And Case 2 is the certain repetition due to the non-monotonic variation of fiber orientation. In this method, it is assumed that the variation of the fiber orientation tensor is linear, i.e., the distribution of the fiber orientation tensor conforms to a multi-segment linear function. In a matter of fact, it is also possible to express the variation of the fiber orientation tensor by some other functions.

Case 1 is shown in the left part of Figure 3(a), the isometric distribution of five data points A to E simulates the shell distribution, L denotes the transverse coordinate span from point A to point E, and L_i ($i = 1, 2, \dots, 7$) denotes the transverse coordinate span of each segment, then the probability of the fiber orientation tensor is expressed as:

$$\begin{cases} P_1 = P(A, E) = L_1/L \\ P_2 = P(E, B) = (L_2 + L_7)/L \\ P_3 = P(B, D) = (L_3 + L_6)/L \\ P_4 = P(D, C) = (L_4 + L_5)/L \end{cases} \quad (12)$$

The cumulative distribution of the fiber orientation after processing is shown in the right part

of Figure 3(a).

Case 2 shown in the left part of Figure 3(b), The four points F to I of the isometric distribution simulate a non-monotonic distribution, L' denotes the transverse coordinate span from point F to point I, and $L_i (i = 8, 9, \dots, 12)$ denotes the transverse coordinate span of each segment, then the probability of the fiber orientation tensor is expressed as:

$$\begin{cases} P_5 = P(F, H) = L_8/L' \\ P_6 = P(H, G) = (L_9 + L_{10} + L_{11})/L' \\ P_7 = P(G, I) = L_{12}/L' \end{cases} \quad (13)$$

Similarly, the corresponding probability cumulative distribution form can be obtained as shown in the right part of Figure 3(b).

Method 2: Summarizing all fiber orientation data.

In this method, all fiber orientation data are pooled together, and resolving the discrepancy along the thickness median approximation symmetry, as the main need, similar to the processing in Method 1. In addition, there is quite an increase in computational volume compared to Method 1.

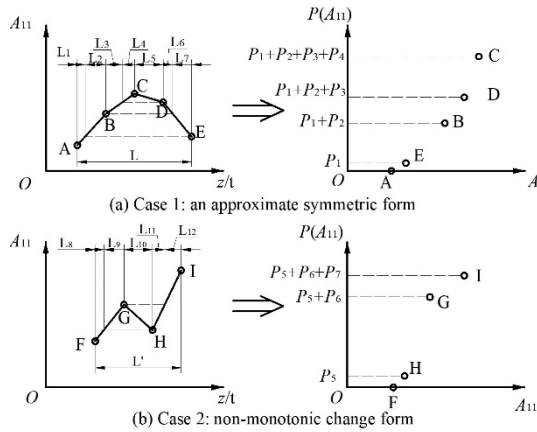


Figure 3 Two forms of distribution for data

RESULTS AND DISCUSSION

Cumulative Distribution Function for Fiber Orientation Versus Data

Compared to short-fiber reinforced thermoplastics, long-fiber reinforced thermoplastics have a wider core region and are more difficult to bias into alignment with the flow direction (Phelps, 2009). A series of long fiber reinforced thermoplastic fiber orientation tensor data measured by Phelps is used to

test the effect of the de-asymmetry method on the fitting results. The values of the fiber orientation tensor A_{11} of the experimentally long fiber-reinforced thermoplastics are uniformly distributed in the direction of their thickness and in a total number of 21. The macroscopic properties of the material are given in Table 1 for all samples, and more details can be found in the literature. The experimental data are arranged from smallest to largest according to the method in the previous section, and the comparison between the experimental data before and after correction and the distribution function is shown in Figure 4.

It can be observed from Figure 4 that there is a good fit between the experimental data processed according to the de-asymmetry method and the CDF, and the corrected fit is also good. R-square is a parameter that indicates the goodness of fit, and SSE refers to Sum of Squared Error. The closer R-square is to 1 or SSE is to 0, the better the result. Thus, both R-square and SSE show a better result than those in the literature (Huang and Zhao, 2020). Two large changes in the slope of the CDF are evident in the form of the experimental data distribution, corresponding to the two peaks of the probability distribution function of the fiber orientation tensor.

Table 1 Material and geometry of LFT samples.

Sample ID	Material	Geometry
PNNLAS3I	MTIPP40G	90 mm long × 80 mm wide ISO plaque
PNNLBF3D	MTI PP30C	180 mm diameter disk

Prediction for Elastic Modulus Versus Experiment

In this section, the prediction of LFT elastic modulus based on fiber orientation distribution function and fiber length distribution and the accuracy of its comparative experimental results are investigated. The mechanical properties of the material are shown in Table 2. Two specimens, the center-gated disk and the ISO -plaque, were fabricated by injection molding, and more details are in the literature (Nguyen et al., 2008).

The performance of materials is usually affected by a variety of factors (Ge et al., 2021; Liang et al., 2021; Mao et al., 2021; Tong et al., 2019). According to the literature (Tucker and Liang, 2001; Budarapu et al., 2019; Alazwari, 2021; Devanathan et al., 2020; Zhang et al., 2019; Zhu et al., 2020; Keshtegar et al., 2021; Wang et al., 2021),

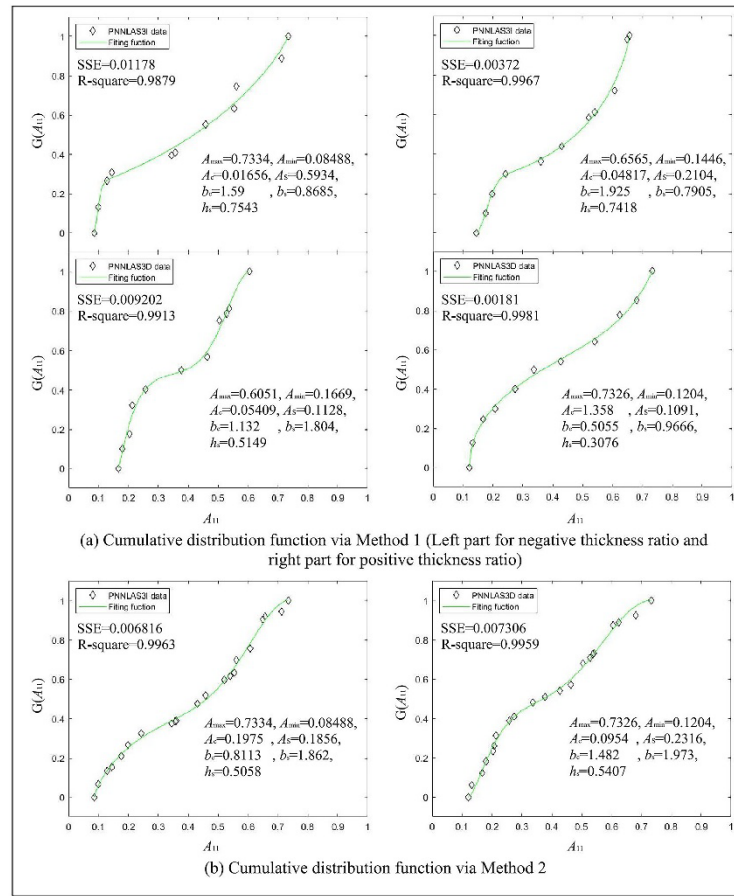


Figure 4 Cumulative distribution function for orientation tensor of samples via Method 1 and 2

some models and methods are described. Usually, the prediction of the elastic modulus of LFT materials requires homogenization, which is generally calculated from the mean value of the fiber length and fiber orientation properties. Therefore, the prediction of the elastic modulus of LFT materials is divided into two main steps, first considering the elastic modulus of the material when the fiber length is aligned unidirectionally to the fibers, and then considering the elastic modulus when the fibers have the actual orientation state. The specific steps are described below.

Table 2 Mechanical properties of materials for injection molded composites components

Material	Diameter (um)	Elastic modulus (GPa)	Poisson ratio	Volume fraction (%)
PP	/	1.5	0.4	80.8
Glass fiber	17.4	73	0.25	19.2

The stiffness matrix of a unidirectional fiber composite considering the fiber length distribution is expressed as :

$$C_{ijkl} = \frac{\int_0^\infty C_{ijkl}^*(l/d)p(l)dl}{\int_0^\infty p(l)dl} \quad (14)$$

where, $C_{ijkl}^*(l/d)$ refers to the stiffness matrix of a unidirectionally aligned fiber composite at a fiber aspect ratio of l/d , $p(l)$ refers to the PDF of the fiber length, which can be expressed in terms of the number-average fiber length or weight average fibers length. In general, since the fiber weight distribution is proportional to the volume, and the process of finding the mean of the length distribution is essentially the mean of the volume.

In this section, the weight distribution of the fiber length is used. And $C_{ijkl}^*(l/d)$ is calculated by The Eshelby-Mori-Tanaka method proposed in the literature (Camacho et al., 1990; Taya and Mura, 1981).

For fiber length calculation, the two-parameter Weibull distribution was chosen to find the average fiber length. The expressions are:

$$p(l) = \frac{c}{b} \left(\frac{l}{b}\right)^{c-1} e^{-\left(\frac{l}{b}\right)^c} \quad (15)$$

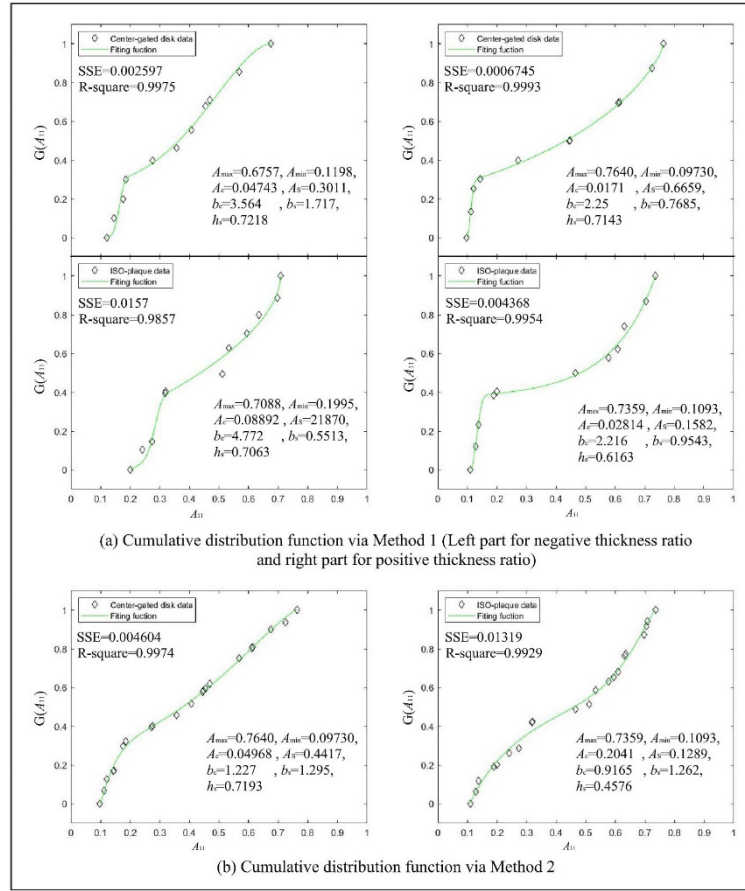


Figure 5 Cumulative distribution function for orientation tensor of center-gated disk and ISO-plaque via Method 1 and 2

where l refers to the fiber length and b, c are the shape parameters.

Subsequently, the orientation averaging method was applied to calculate the stiffness matrix of the composite in the actual fiber orientation state (Camacho et al., 1990), with the expression:

$$\begin{aligned} \bar{C}_{ijkl} = & B_1 A_{ijkl} + B_2 (A_{ij} \delta_{kl} + A_{kl} \delta_{ij}) \\ & + B_3 (A_{ik} \delta_{jl} + A_{il} \delta_{jk} + A_{jl} \delta_{ik} + A_{jk} \delta_{il}) \\ & + B_4 \delta_{ij} \delta_{kl} + B_5 (\delta_{ik} \delta_{jl} + \delta_{il} \delta_{jk}) \end{aligned} \quad (16)$$

where the parameters $B_i (i = 1, 2, \dots, 5)$ refer to the invariant of the unidirectional arrangement of the transverse isotropic composite stiffness matrix, which is given in the literature (Camacho et al., 1990).

Table 3 Number-average and weight-average lengths determined from the Weibull's distributions versus those determined from data.

	\bar{L}_n (mm)	\bar{L}_n^{weib} (mm)	\bar{L}_w (mm)	\bar{L}_w^{weib} (mm)
IOS-plaque	1.04	1.05	1.83	1.71
Center-gated disk	1.33	1.34	2.18	2.28

Table 3 extracted from the literature (Nguyen et al., 2008) give the experimental number and weight mean lengths and the number and weight mean lengths

obtained by fitting the two-parameter Weibull distribution, and it can be seen that the fitted mean values are very close to the experimental values and can effectively represent the fiber length distribution. However, some of the details of the variations still do not fit well.

Figure 5 shows the fitted curves obtained according to the de-asymmetry method, and it can be seen that the corrected experimental data fit the fitted function very well. $SSE=0.01655$, $R\text{-square}=0.9914$ for center-gated disk and $SSE=0.01478$, $R\text{-square}=0.9923$ for ISO-plaque in the fit results of unprocessed data. It is clear that the de-asymmetry method performs even better. What's more, Method 2 outperformed Method 1 in the center-gated disk data, while Method 1 outperformed Method 2 in ISO-plaque data. The average values of the fiber orientation tensor obtained from the function are shown in Table 4.

The stiffness matrix of the composite specimens was calculated using micromechanical modeling software. And the two-parameter Weibull distribution based on the fiber length and the generalized distribution function of the fiber orientation tensor predict the elastic modulus of the center-gated disk and IOS-plaque ($\bar{E}_{11}, \bar{E}_{22}$), as shown in Tables 5 and 6.

Table 4 Parameters and elastic modulus with thickness-average orientation tensor for center-gated disk and ISO-plaque

	\bar{L}_w^{weib} (mm)	D (um)	Method 1		Method 2		Raw data	
			\bar{A}_{11}	\bar{A}_{22}	\bar{A}_{11}	\bar{A}_{22}	\bar{A}_{11}	\bar{A}_{22}
Center-gated disk	2.28	17.4	0.383	0.592	0.382	0.593	0.380	0.592
ISO-plaque	1.71	17.4	0.435	0.535	0.433	0.537	0.445	0.527

The comparison of the predicted values of the elastic modulus of the center-gated disk and IOS-plaque with the experimental results and predicted values in literature (Nguyen et al., 2008) is shown in Tables 5 and 6. The standard deviation (SDV) of the experimental results and the predicted values and the relative error (RE) of the predicted values with respect to the experimental results are indicated in the tables.

And the results of the predicted elastic moduli based on other methods and their relative errors are also listed.

In Tables 5 and 6, it can be seen that the experimental results have a good correlation with the predicted values calculated based on the de-asymmetry method, which proves the reliability of the LFT elastic modulus prediction model. And the results obtained by the de-asymmetry method are closer to the experimental values than those obtained by other methods. The mutation of the cumulative function due to the asymmetric fiber orientation. It, the result E_{11} obtained by Weibull's FLD and GDF's FOD in Table 6, could be possible that the asymmetry causes a closer result to experimental data. It can be seen that the de-asymmetry method shows a positive effect on the accurate prediction of the elastic modulus of materials.

Table 5 Predictions versus experimental data for center-gated disk

Experimental data		Predictions			
		Experimental FLD and RSC's FOD	Weibull's FLD and GDF's FOD	Weibull's FLD and GDF's FOD with Method 1	Weibull's FLD and GDF's FOD with Method 2
\bar{E}_{11}	5318 ^{a)}	5942 ^{a)}	5041	5078	5062
(MPa)	SDV=122.6	RE=11.7%	RE=-5.2%	RE=-4.5%	RE=-4.8%
\bar{E}_{22}	7521 ^{a)}	5826 ^{a)}	7335	7346	7366
(MPa)	SDV=16.3	RE=-22.5%	RE=-2.5%	RE=-2.3%	RE=-2.1%

^{a)} Taken from Ref. (Nguyen et al., 2008).

Table 6 Predictions versus experimental data for ISO-plaque

Experimental data		Predictions			
		Experimental FLD and RSC's FOD	Weibull's FLD and GDF's FOD	Weibull's FLD and GDF's FOD with Method 1	Weibull's FLD and GDF's FOD with Method 2
\bar{E}_{11}	6063 ^{a)}	5361 ^{a)}	5591	5491	5469
(MPa)	SDV=181.1	RE=-11.6%	RE=-7.8%	RE=-9.4%	RE=-9.8%
\bar{E}_{22}	7211 ^{a)}	6377 ^{a)}	6463	6545	6563
(MPa)	SDV=479	RE=-11.6%	RE=-10.4%	RE=-9.2%	RE=-9.0%

^{a)} Taken from Ref. (Nguyen et al., 2008).

CONCLUSIONS

In this paper, a de-asymmetry method of fiber orientation PDF was proposed to obtain the homogenized fiber orientation tensor and used to predict the mechanical properties of injection molded composites. The important conclusions of this paper are summarized as follows:

(1) A smooth segmented linear function of fiber orientation was proposed based on the relationship between the effective thickness in the thickness direction and the probability density of the fiber orientation tensor. The shell thickness ratio was introduced to describe the microstructure form of injection molded composites, and the form of the fiber

orientation PDF was obtained by considering the two-parameter Weibull distribution.

(2) The idea that the ratio of the thicknesses occupied when the fiber orientation tensor changes represent the probability density of the fiber orientation tensor was carried out. And considering the asymmetry and non-monotonicity of the fiber orientation distribution, the de-asymmetry method was proposed based on the idea. The CDF has better goodness of fit compared with the experimental results in the literature.

(3) The homogenized fiber orientation tensor obtained by the de-asymmetry method was applied to the prediction of mechanical properties of injection molded composites, and the obtained predictions correlated well with the elastic modulus obtained from experimental data.

(4) The PDF of the fiber orientation tensor was proposed, and it can be assumed that the variation of the fiber orientation tensor conforms to other functions than linear variation. Besides, there are various expression functions for the angular distribution of fiber orientation in existing studies. The relationship between the fiber orientation tensor and the angle of fiber orientation can be combined to describe the microstructure of injection molded composites more clearly. In future work, it seems feasible to combine these two and calculate the mechanical properties of the material in terms of the overall angular distribution of the fibers of the material.

REFERENCES

- Advani, S.G., and Tucker, C.L., "The use of tensors to describe and predict fiber orientation in short fiber composites", *J. Rheol.*, Vol. 31, pp. 751–784 (1987).
- Alazwari, M.A., "Non-probabilistic models for in-plane elastic properties of cellular hexagonal honeycomb cores involving imprecise parameters", *Adv. Mech. Eng.*, Vol. 13 No. 8, pp.1-10 (2021).
- Budarapu, P.R. et al., "Multiscale modeling of material failure: theory and computational methods", *Adv. Appl. Mech.*, Vol. 52, pp.1-103 (2019).
- Camacho, C.W. et al., "Stiffness and thermal expansion predictions for hybrid short-fiber composites", *Polym. Compos.*, Vol. 11, pp.229-239 (1990).
- Chang, B. et al., "Effects of temperature and fiber orientation on the tensile behavior of short carbon fiber reinforced PEEK composites", *Polym. Compos.*, Vol. 42, pp. 597-607 (2020).
- Chen, C.H., and Cheng, C.H., "Effective elastic moduli of misoriented short-fiber composites", *Int. J. Solids Struct.*, Vol. 33, pp.2519-2539 (1996).
- Chin, W.K. et al., "Effects of fiber length and orientation distribution on the elastic modulus of short fiber reinforced thermoplastics", *Polym. Compos.*, Vol. 9, pp.27-35 (1988).
- Devanathan, C., et al., "Predicting the tensile strength of metal matrix composites joined by friction stir welding and optimization of parameters using firefly algorithm", *J. Chin. Soc. Mech. Eng.*, Vol. 41 No. 4, pp. 513-520 (2020).
- Folgar, F., and Tucker, C.L., "Orientation behavior of fibers in concentrated suspensions", *J. Reinf. Plast. Compos.*, Vol. 3(2),98-119 (1984).
- Friedrich, K., "Mesoscopic aspects of polymer composites: Processing, structure and properties", *J. Mater. Sci.*, Vol. 33, pp. 5535–5556 (1998).
- Fu, S.Y., and Lauke, B., "An analytical characterization of the anisotropy of the elastic modulus of misaligned short-fiber-reinforced polymers", *Compos. Sci. Technol.*, Vol. 58, pp.1961-1972 (1998).
- Ge H.Y., et al., "Effect of fisheye failure on material performance inducing error circle under high cycles", *Int. J. Damage Mech.*, Vol.30(10), pp.1524-1541 (2021).
- Hessman, P.A. et al., "Microstructural analysis of short glass fiber reinforced thermoplastics based on x-ray micro-computed tomography", *Compos. Sci. Technol.*, Vol. 183, 107752 (2019).
- Huang, D.Y., and Zhao, X.Q., "A generalized distribution function of fiber orientation for injection molded composites", *Compos. Sci. Technol.*, Vol. 188, 107999 (2020).
- Jeffery, G.B., "The motion of ellipsoidal particles immersed in a viscous fluid", *Proc. R. Soc. London, Ser. A*, Vol. 102, pp.161-179 (1922).
- Kebir, T., et al., "Numerical study of fatigue damage under random loading using Rainflow cycle counting.", *Int. J. Mater. Struct. Integr.*, Vol. 12(3), pp. 408-418 (2021).
- Keshtegar B., et al., "Optimization of buckling load for laminated composite plates using adaptive Kriging-improved PSO: A novel hybrid intelligent method", *Def. Technol.*, Vol. 17(1), pp. 85-99(2021).
- Laspalas, M. et al., "Application of micromechanical models for elasticity and failure to short fibre reinforced composites. Numerical implementation and experimental validation", *Comput. Struct.*, Vol. 86, pp.977-987 (2008).
- Liang Z.Q., et al., "Universal grey number theory for the uncertainty presence of wiper structural system", *Assembly Autom.*, Vol.41(1), pp.55-70(2021).
- Liu X.T., et al., "Evaluation and prediction of material fatigue characteristics under impact loads: review and prospects", *Int. J. Mater. Struct. Integr.*, Vol. 13(2), pp.251-277(2022).
- Lu, Y., and Liaw, P.K., "Effect of particle orientation in silicon-carbide particulate reinforced aluminum matrix composite extrusions on ultrasonic velocity measurement", *J. Compos. Mater.*, Vol. 29 No. 8, pp.1096-1116 (1995).
- Mao K. et al., "Reliability analysis for mechanical parts considering hidden cost via the modified quality loss model", *Qual. Reliab. Eng. Int.*, Vol.37(6), pp.1373-1395(2021).
- Mishurova, T. et al., "Evaluation of the probability density of inhomogeneous fiber orientations by computed tomography and its application to the calculation of the effective properties of a fiber-reinforced composite", *Int. J. Eng. Sci.*, Vol. 122, pp.14-29 (2018).
- Nguyen, B.N. et al., "Fiber length and orientation in long-fiber injection-molded thermoplastics - part I: modeling of microstructure and elastic

- properties”, *J. Compos. Mater.*, Vol. 42, pp.1003-1029 (2008).
- Ning, H.B. et al., “A review of long fibre-reinforced thermoplastic or long fibre thermoplastic (LFT) composites”, *Int. Mater. Rev.*, Vol. 65, pp. 164-188 (2019).
- Pettermann, H.E. et al., “Some direction-dependent properties of matrix-inclusion type composites with given reinforcement orientation distributions”, *Composites, Part B*, Vol. 28, pp.253-265 (1997).
- Phelps, J.H., “Processing-microstructure models for short- and long-fiber thermoplastic composites”, Ph.D. thesis, University of Illinois at Urbana-Champaign, Urbana (2009).
- Phelps, J.H., and Tucker, C.L., “An anisotropic rotary diffusion model for fiber orientation in short- and long-fiber thermoplastics”. *J. Non-Newtonian Fluid Mech.*, Vol. 156, pp.165-176 (2009).
- Sevostianov, L. et al., “Effective viscoelastic properties of short-fiber reinforced composites”, *Int. J. Eng. Sci.*, Vol. 100, pp.61-73 (2016).
- Sevostianov, L., and Kachanov, M., “Modeling of the anisotropic elastic properties of plasma-sprayed coatings in relation to their microstructure”, *Acta Mater.*, Vol. 48, pp.1361-1370 (2000).
- Sharma, B.N. et al., “Reliability in the characterization of fiber length distributions of injection molded long carbon fiber composites”, *Polym. Compos.*, Vol. 39, pp.4594-4604 (2017).
- Taya, M., and Mura, T., “On stiffness and strength of an aligned short-fiber reinforced composite containing fiber-end cracks under uniaxial applied stress”, *J. Appl. Mech.*, Vol. 48, pp.361-367 (1981).
- Tong J.C., et al., “Research on Random Load Characteristic Based on Mixture Distribution Model”, *J. Test. Eval.*, Vol.47(1), 20170131(2019).
- Truckenmüller, F., and Fritz, H.G., “Injection molding of long fiber-reinforced thermoplastics: A comparison of extruded and pultruded materials with direct addition of roving strands”, *Polym. Eng. Sci.*, Vol. 31, pp. 1316–1329 (1991).
- Tseng, H.C. et al., “An objective tensor to predict anisotropic fiber orientation in concentrated suspensions”, *J. Rheol.*, Vol. 60 No. 2, pp.215-224 (2016).
- Tseng, H.C. et al., “Comparison of recent fiber orientation models in injection molding simulation of fiber reinforced composites”, *J. Thermoplast. Compos. Mater.*, Vol. 33, pp.35-52 (2020).
- Tucker, C.L., and Liang, E., “Stiffness predictions for unidirectional short-fiber composites: Review and evaluation”, *Compos. Sci. Technol.*, Vol. 59, pp.655-571 (2001).
- Viana, C.O., et al., “Fatigue assessment based on hot-spot stresses obtained from the global dynamic analysis and local static sub-model”, *Int. J. Mater. Struct. Integr.*, Vol. 12(1), pp.31-47(2022).
- Wang, J. et al., “An objective model for slow orientation kinetics in concentrated fiber suspensions: Theory and rheological evidence”, *J. Rheol.*, Vol. 52, pp.1179-1200 (2008).
- Wang S.C., et al., “Fatigue life prediction of composite suspension considering residual stress and crack propagation”, *Proc. Inst. Mech. Eng., Part D*, online(2022).
- Wang, Y.H., et al., “Improved fatigue failure model for reliability analysis of mechanical parts inducing stress spectrum”, *Proc. Inst. Mech. Eng., Part O*, Vol. 235(6), pp. 973-981 (2021).
- Zhang, H., et al., “Type synthesis of fully-isotropic 2t3r 5-dof hybrid mechanisms”, *J. Chin. Soc. Mech. Eng.*, Vol. 40 No. 3, pp. 307-314 (2019).
- Zhu, S.P., et al., “Dynamic buckling optimization of laminated aircraft conical shells with hybrid nanocomposite material”, *Aerosp. Sci. Technol.*, Vol. 98, 1056565(2020).

註塑成型復合材料纖維取向分布函數的去非對稱方法

職山傑 劉和劍
蘇州大學應用技術學院

楊錫洲 劉新田
上海工程技術大學

摘要

纖維取向是決定註塑復合材料力學性能的關鍵因素。因此，準確描述纖維取向對註塑復合材料性能評估有重要作用。基於厚度方向有效厚度與纖維取向張量的概率密度之間的關係，提出了纖維取向的平滑分段線性函數用以得到纖維取向張量累積分布函數。考慮到纖維取向分布的近似對稱性和非單調性，提出了去非對稱化方法。與文獻中的實驗結果相比，累計分布函數具有良好的擬合優度，並且實驗結果與本方法得到的纖維取向張量預測的彈性模量有良好的相關性。可為後續基於纖維取向張量厚度分布的研究提供參考依據。